Supporting information for

Rational synthesis of an ultra-stable Zn(II) coordination polymer based on a new tripodal pyrazole ligand for highly sensitive and selective detection of Fe^{3+} and $Cr_2O_7^{2-}$ in aqueous media

Shi-Hui Zhang,‡ Shu-Yu Zhang,‡ Jing-Rong Li, Zhen-Qi Huang, Jing Yang, Ke-Fen Yue* and Yao-Yu Wang

Key Laboratory of Synthetic and Natural Functional Molecule of the Ministry of Education, National Demonstration Center for Experimental Chemistry Education (Northwest University), Shaanxi Key Laboratory of Physico-Inorganic Chemistry, College of Chemistry and Materials Science, Northwest University, Xi'an 710127, China

Table S1 List of several reported Zn(II) coordination polymers for luminescent sensing

Ligands type	Chemical Stability	Applications	Ref.
A carboxylate ligand	Poor water stability	Sensing $Cr_2O_7^{2-}$, CrO_4^{2-} and Fe^{3+} in DMF/H_2O or DMA/H_2O solutions	1
A carboxylate ligand	Poor water stability	Sensing 2,4,6-trinitrophenol in DMF solution	2
A carboxylate ligand	Poor water stability	Sensing tetrabromobisphenol A in EtOH solution	3
A carboxylate ligand	Poor water stability	Sensing Fe^{3+}, Cu^{2+} and nitrobenzene in DMF solution	4
A carboxylate ligand	Poor water stability	Sensing 2,4,6-trinitrophenol in DMF media	5
A carboxylate ligand	Poor water stability	Sensing Fe^{3+} and trinitrotoluene in DMF solution	6
A carboxylate ligand	Poor water stability	Sensing nitroaromatics and Fe^{3+} in DMF solution	7
A carboxylate ligand & a flexible pyridine-based ligands	Poor water stability	Sensing Cr^{3+}, CrO_4^{2-}, $Cr_2O_7^{2-}$, 4-nonylphenol, and 2,4,6-trinitrophenol in DMF solution	8
A carboxylate ligand & a rigid pyridine-based ligand	Good water stability	Sensing MnO_4^{-}, $Cr_2O_7^{2-}$ and CrO_4^{2-} in aqueous media	9
A carboxylate ligand & a rigid pyridine-based ligand	Good water stability	Sensing Cr^{3+}, $Cr_2O_7^{2-}$, and *p*-nitrotolune in aqueous media	10
A carboxylate ligand & the rigid phen	Good water stability	Sensing CrO_4^{2-} and $Cr_2O_7^{2-}$ in aqueous media	11
A carboxylate ligand & the rigid phen	Good water stability	Sensing uric acid in aqueous media	12
A sulfonate ligand & a flexible azole-based ligands	Good water stability	Sensing Fe^{3+} in aqueous media	13
A carboxylate ligand & a flexible azole-based ligand	Good water stability	Sensing glyoxal and $Cr_2O_7^{2-}$ in aqueous media	14
A carboxylate ligand & a rigid pyridine-based ligand	Good water stability	Sensing MnO_4^{-} and $Cr_2O_7^{2-}$ in aqueous media	15
A carboxylate ligand & a rigid azole/pyridine-based ligands	Good water stability	Sensing 2,6-dichloro-4-nitroaniline, Fe^{3+}, CrO_4^{2-}, and $Cr_2O_7^{2-}$ in aqueous media	16

A carboxylate ligand & an azole ligand	Good solvent stability	Sensing aniline and benzaldehyde in DMF and $Cr_2O_7^{2-}$ and CrO_4^{2-} in aqueous media	17
A carboxylate ligand & a rigid pyridine-based ligand	Good solvent stability	Sensing 2,4,6-trinitrophenol in DMF and Fe^{3+} and Al^{3+} in aqueous media	18
A carboxylate ligand & a rigid tritopic pyridine-based ligand	Good water and pH stability	Sensing acetylacetone in aqueous media	19
A carboxylate ligand & a rigid pyridine-based ligand	Good water and pH stability	Sensing $Cr_2O_7^{2-}$ and CrO_4^{2-} in aqueous media	20
A carboxylate ligand & a semi-rigid azole/pyridine-based ligands	Good water and pH stability	pH sensing in aqueous media	21
A carboxylate ligand & an azole ligand	Good water and pH stability	Sensing Fe^{3+}, Al^{3+}, SiF_6^{2-}, $Cr_2O_7^{2-}$, nitrofurantoin, and nitrofurazone in aqueous media	22
A carboxylate ligand & a rigid pyridine-based ligand	Good water and pH stability	Sensing $Cr_2O_7^{2-}$, CrO_4^{2-} and 2,4,6-trinitrophenol in aqueous media	23
Flexible azole-based ligands	Good water and pH stability	Sensing $Cr_2O_7^{2-}/CrO_4^{2-}$ in aqueous media	24
A carboxylate ligand & a rigid tritopic pyrazole-based ligand	**Good water, thermal, and pH stability**	**Sensing Fe^{3+} and $Cr_2O_7^{2-}$ in aqueous media**	**This work**

Table S2 Crystal data and structure refinements for complex **1**

Complex	**1**
Molecular Formula	$C_{24}H_{16}ZnN_6O_6$
Formula Weight	547.78
Temperature (K)	296(2)
Crystal System	monoclinic
Space Group	$P2_1/c$
a (Å)	16.0291(19)
b (Å)	8.3132(10)
c (Å)	17.158(2)
α (°)	90
β (°)	91.520(2)

γ (°)	90
V (Å^3)	2285.5(5)
Z	4
Dc (g·cm^{-3})	1.598
F(000)	1112.0
[R(int)]	0.0282
GOF on F^2	1.041
R_1[a] [I>2σ(I)]	0.0348
wR_2[b] [all data]	0.0911

$^aR_1 = \Sigma||F_o| - |F_c||/\Sigma|F_o|$. $^b\mathrm{w}R_2 = [\Sigma w(F_o^2 - F_c^2)^2/\Sigma w(F_o^2)^2]^{1/2}$

Table S3 Selected bond distances (Å) and angles (°) for complex **1**

1			
Zn(1)-O(1)	1.9577(17)	Zn(1)-N(1)	2.012(2)
Zn(1)-O(5)	2.0084(17)	Zn(1)-O(6)	2.3702(19)
Zn(1)-N(3)	1.994(2)	O(1)-Zn(1)-O(6)	154.46(7)
O(5)-Zn(1)-O(6)	58.85(7)	O(5)-Zn(1)-N(1)	116.85(9)
N(1)-Zn(1)-O(6)	96.06(8)	N(3)-Zn(1)-O(5)	128.76(9)
N(3)-Zn(1)-N(1)	107.02(9)	N(3)-Zn(1)-O(6)	92.68(8)
O(1)-Zn(1)-O(5)	97.43(7)	O(1)-Zn(1)-N(1)	103.98(8)
O(1)-Zn(1)-N(3)	96.36(8)		

Table S4 Kinetic parameters of the complex **1**

Complex	β (K·min^{-1})	T_p (K)	Kissinger's method			Ozawa–Doyle's method	
			E_K§ (kJ·mol^{-1})	lnA_K§ (s^{-1})	R_K	E_O§§ (kJ·mol^{-1})	R_O§§
1	2	696.56	214.80	13.37	0.9996	215.50	0.9994
	5	712.17					
	8	721.17					
	10	768.83					

§ subscript K represents Kissinger's method

§§ subscript O represents Ozawa–Doyle's method

Table S5 Thermodynamic parameters of the complex **1**

Complex	β K·min^{-1}	$\Delta G^{\neq}$ kJ·mol^{-1}	$\Delta H^{\neq}$ kJ·mol^{-1}	$\Delta S^{\neq}$ J·mol^{-1}·K^{-1}	T_p K
1	2	313.25	209.01	-149.66	696.56
	5	315.58	208.88	-149.83	712.17
	8	316.93	208.80	-149.93	721.17
	10	324.06	208.41	-150.43	768.83
Mean		317.46	208.77	-149.96	724.68

Table S6 Comparison of the Stern-Volmer constant (K_{SV}) used for sensing Fe^{3+} with other coordination polymers

Materials	Medium	Ksv (M^{-1})	Ref.
$Eu_2(MFDA)_2(HCOO)_2(H_2O)_6$	DMF	1.58×10^3	25
$[Eu_2(L_2)_{1.5}(H_2O)_2EtOH]\cdot DMF$	DMF	2.94×10^3	26
Tb-DSOA	H_2O	3.54×10^3	27
$Ln(cpty)_3$	H_2O	4.10×10^3	28
$[Zr_6O_4(OH)_4(C_8H_2O_4S_2)_6]\cdot DMF\cdot 18H_2O$	H_2O	4.40×10^3	29
Eu^{3+}@MIL-53-COOH·(Al)	H_2O	5.12×10^3	30
Bis(rhodamine)-1	CH_3CN	7.50×10^3	31
Eu-BPDA	H_2O	1.25×10^4	32
$[La(TPT)(DMSO)_2]\cdot H_2O$	EtOH	1.36×10^4	33
$[Zn(tpb)(Hbtc)]_n$	H_2O	1.57×10^4	**This work**
BUT-15	H_2O	1.66×10^4	34
Benzimidazole-based sensor	H_2O	8.51×10^4	35

Table S7 Comparison of the Stern-Volmer constant (*K*sv) used for sensing $Cr_2O_7^{2-}$ with other coordination polymers.

Materials	Luminescent substrates	Medium	*K*sv (M^{-1})	Ref.
$\{[Cd(L)(SDBA)(H_2O)]\cdot 0.5H_2O\}_n$	$Cr_2O_7^{2-}$	H_2O	4.97×10^3	36
$\{[Cd(L)(BPDC)]\cdot 2H_2O\}_n$	$Cr_2O_7^{2-}$	H_2O	6.40×10^3	36
$Zn_2(ttz)H_2O$	$Cr_2O_7^{2-}$	H_2O	2.19×10^3	24
Zn(btz)	$Cr_2O_7^{2-}$	H_2O	4.23×10^3	24
Eu^{3+}@MIL-121	$Cr_2O_7^{2-}$	H_2O	4.34×10^3	37
$\{[Zn_3(tza)_2(\mu_2\text{-}OH)_2(H_2O)_2]\cdot H_2O\}_n$	$Cr_2O_7^{2-}$	H_2O	5.02×10^3	38
$[Zn_2(TPOM)(BDC)_2]\cdot 4H_2O$	$Cr_2O_7^{2-}$	DMF	7.59×10^3	8
$Eu_2(H_2O)(DCPA)_3$	$Cr_2O_7^{2-}$	H_2O	8.70×10^3	39
$[Tb(TATAB)(H_2O)_2]\cdot NMP\cdot H_2O$	$Cr_2O_7^{2-}$	H_2O	1.11×10^4	40
$[Zn(tpb)(Hbtc)]_n$	$Cr_2O_7^{2-}$	H_2O	9.69×10^3	**This work**

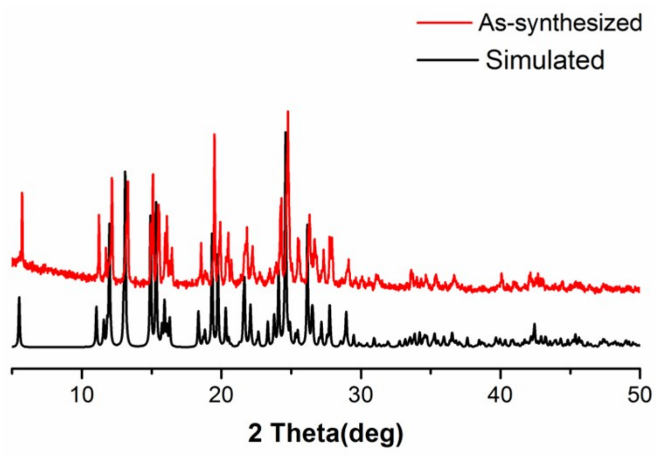

Fig. S1 PXRD pattern of complex **1** simulated from the X-ray single-crystal data and as synthesized products.

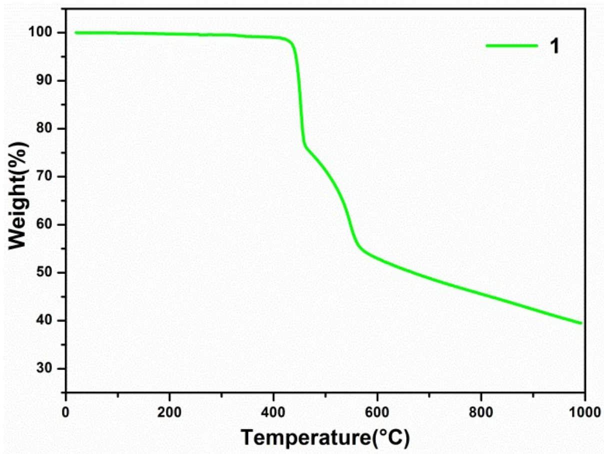

Fig. S2 TGA plot of complex **1**.

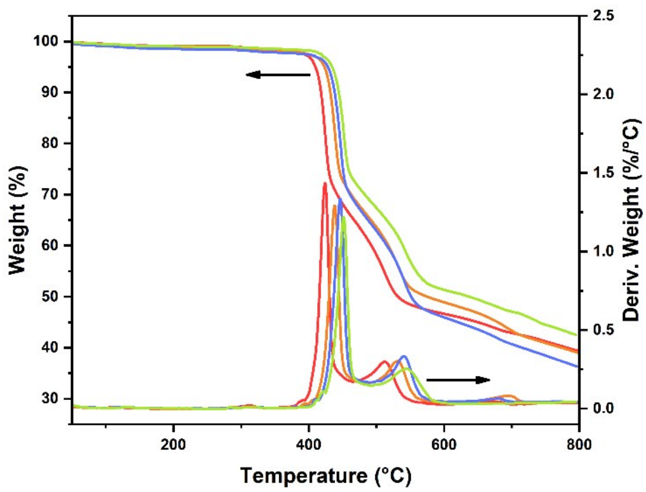

Fig. S3 TGA and DTG curves of **1** at heating rates of 2 (red), 5(orange), 8(blue), and 10 (green) K min^{-1}.

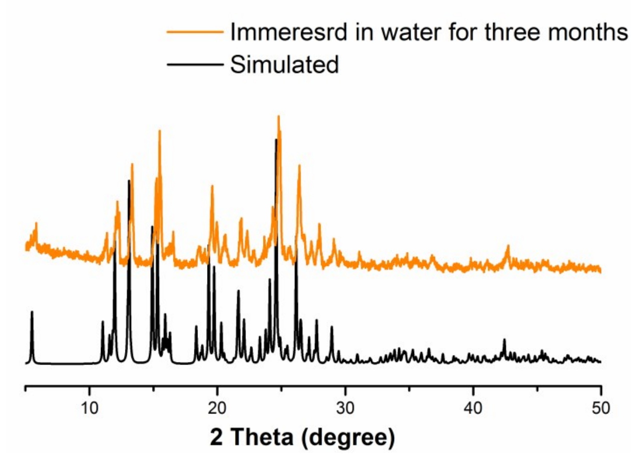

Fig. S4 PXRD pattern of **1** immersed in water at room temperature for three months.

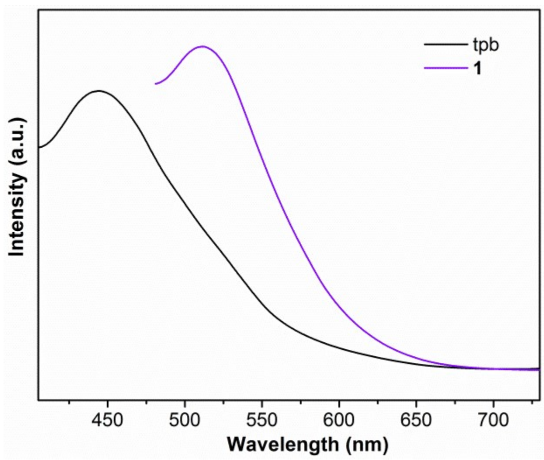

Fig. S5 Emission spectra of **1** and tpb in the solid state at room temperature.

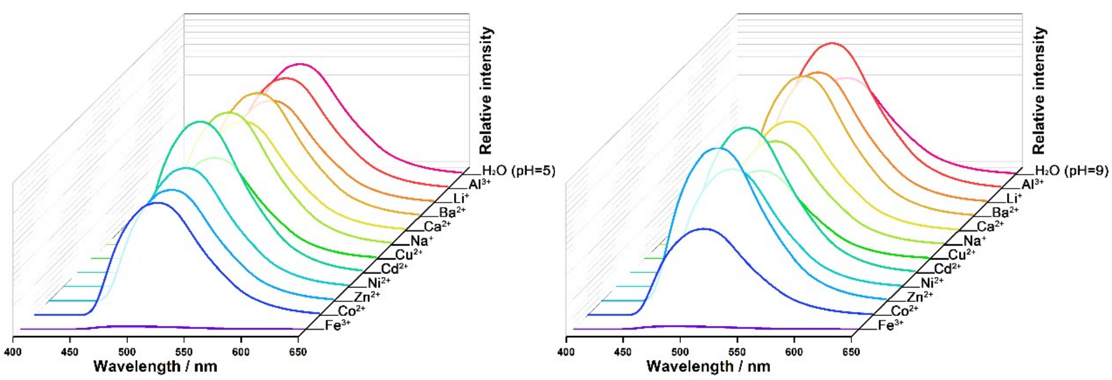

Fig. S6 Luminescence spectra of **1** in various cations aqueous solutions (0.01 M) with different pH values (left: pH = 5; right: pH = 9).

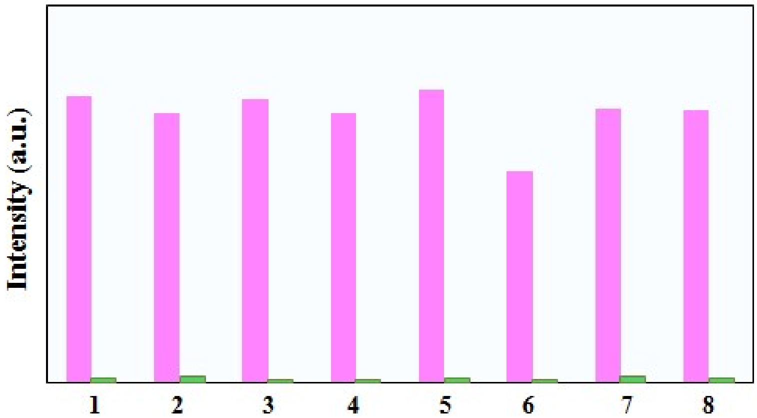

Fig. S7 Luminescence intensity of **1** dispersed in water with the addition of different mixed ions (0.01 M) (1: Al^{3+}/Ba^{2+}; 2: Al^{3+}/Ca^{2+}; 3: Zn^{2+}/Cd^{2+}; 4: Cu^{2+}/Co^{2+}; 5: Zn^{2+}/Cu^{2+}; 6: Cd^{2+}/Co^{2+}; 7: Li^{+}/Ni^{2+}; 8: Ba^{2+}/Ca^{2+}) and Fe^{3+} incorporated systems (0.01 M).

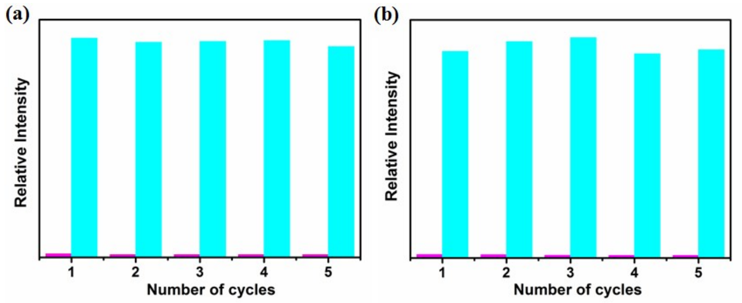

Fig. S8 Multiple cycles for the luminescence quenching of **1** (magenta) by Fe^{3+} (a) and $Cr_2O_7^{2-}$ (b); and recovery after washing by H_2O for several times (cyan).

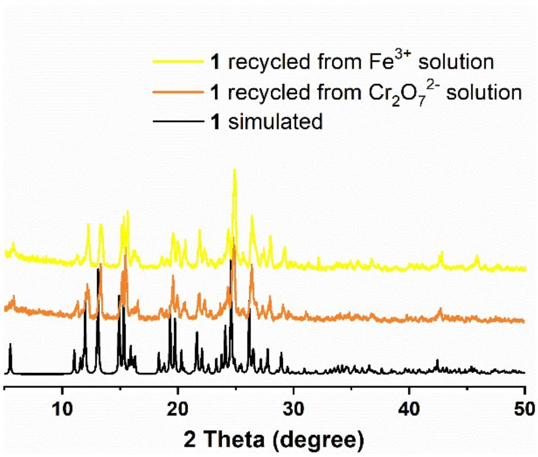

Fig. S9 PXRD patterns of **1** treated by multiple cycles for the luminescence quenching by Fe^{3+} and $Cr_2O_7^{2-}$.

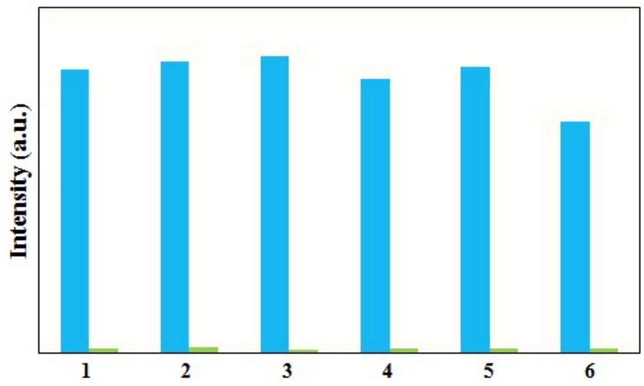

Fig. S10 Luminescence intensity of **1** dispersed in water with the addition of different mixed ions (0.01 M) (1: $NO_3^-/C_2O_4^{2-}$; 2: Cl^-/SCN^-; 3: SO_4^{2-}/Cl^-; 4: SO_4^{2-}/NO_3^-; 5: $Br^-/C_2O_4^{2-}$; 6: $Br^-/C_2O_4^{2-}$) and $Cr_2O_7^{2-}$ incorporated systems (0.01 M).

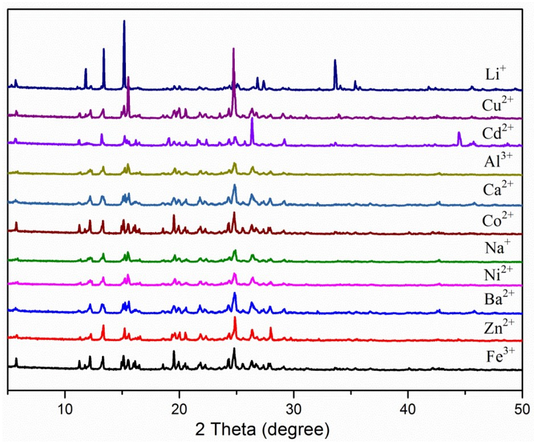

Fig. S11 The PXRD patterns of **1** after cations sensing experiments in aqueous solutions of $M(NO_3)_n$ (M = Li^+, Cu^{2+}, Cd^{2+}, Al^{3+}, Ca^{2+}, Co^{2+}, Na^+, Ni^{2+}, Ba^{2+}, Zn^{2+}, and Fe^{3+}).

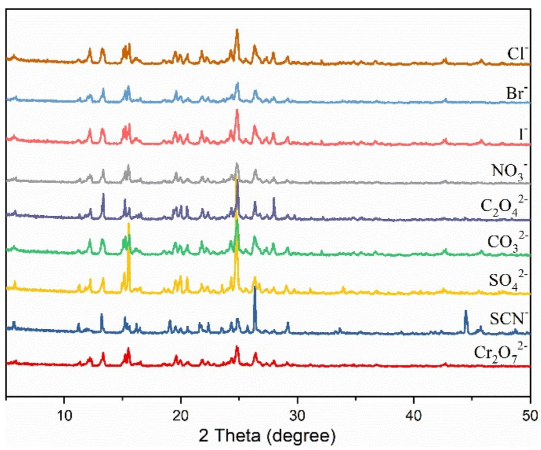

Fig. S12 The PXRD patterns of **1** after anions sensing experiments in aqueous solutions of $K_n(A)$ (A = Cl^-, Br^-, I^-, NO_3^-, $C_2O_4^{2-}$, CO_3^{2-}, SO_4^{2-}, SCN^-, and $Cr_2O_7^{2-}$).

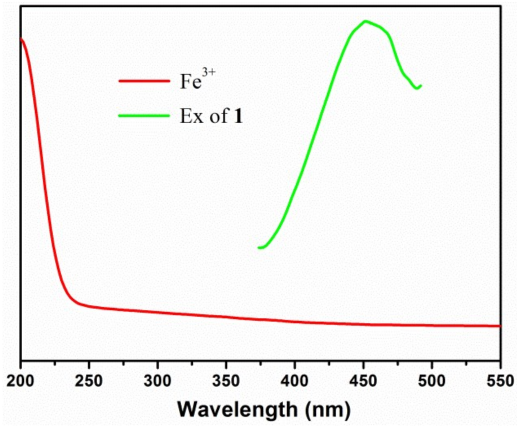

Fig. S13 UV-Vis absorption spectra of $Fe(NO_3)_3$ aqueous solutions and the excitation spectrum of **1**.

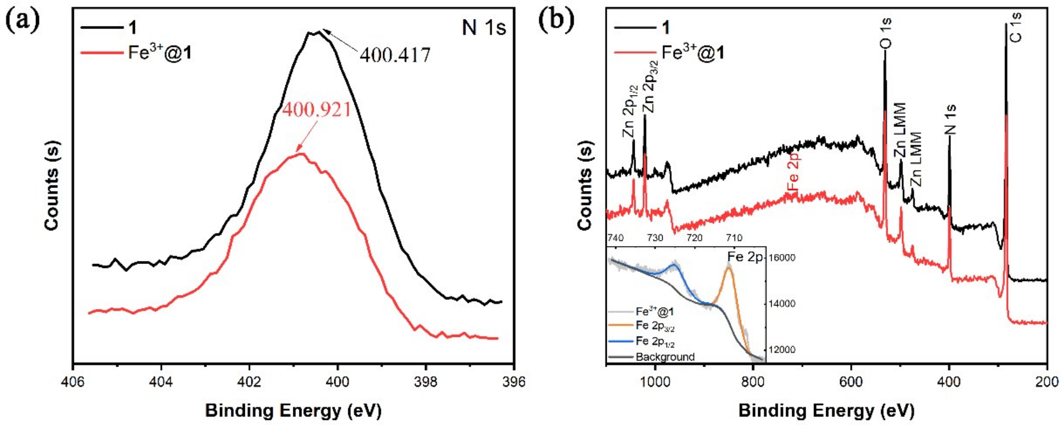

Fig. S14 (a) The N 1s XPS spectra of **1** (black) and Fe^{3+}@**1** (red); (b) Wide XPS spectra of **1** (black) and Fe^{3+}@**1** (red). (Inset: Fe 2p XPS spectra of Fe^{3+}@**1**)

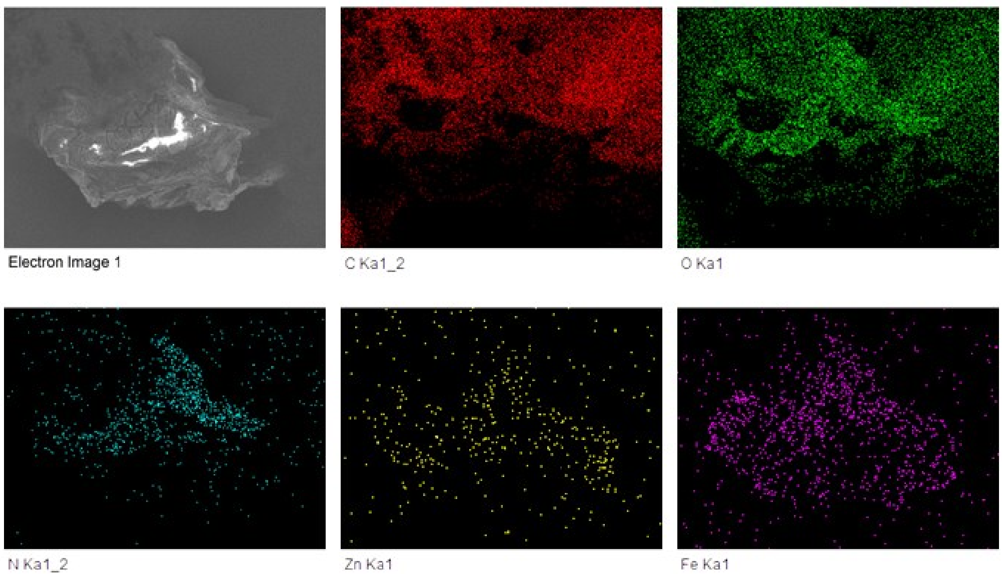

Fig. S15 EDX mapping of Fe^{3+}@**1**.

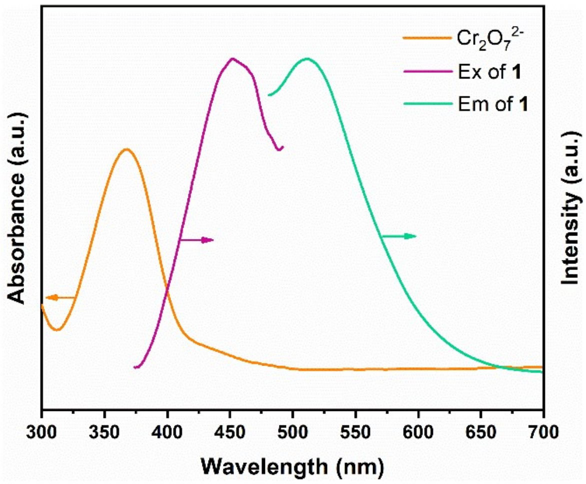

Fig. S16 UV-Vis absorption spectra of $K_2Cr_2O_7$ aqueous solutions together with the excitation and emission spectra of **1**.

References

1 W. H. Huang, J. Z. Li, T. Liu, L. S. Gao, M. Jiang, Y. N. Zhang and Y. Y. Wang, *RSC Adv.*, 2015, **5**, 97127–97132.

2 H. He, D. Y. Zhang, F. Guo and F. Sun, *Inorg. Chem.*, 2018, **57**, 7314–7320.

3 X. lei Zhang, S. mei Li, S. Chen, F. Feng, J. quan Bai and J. rong Li, *Ecotoxicol. Environ. Saf.*, 2020, **187**, 109821.

4 D. Wu, J. Liu, J. Jin, J. Cheng, M. Wang, G. Yang and Y. Y. Wang, *Cryst. Growth Des.*, 2019, **19**, 6774–6783.

5 S. Xing, Q. Bing, H. Qi, J. Liu, T. Bai, G. Li, Z. Shi, S. Feng and R. Xu, *ACS Appl. Mater. Interfaces*, 2017, **9**, 23828–23835.

6 J. K. Wang, X. W. Wang, Z. S. Wang, L. S. Yao, L. Z. Niu, Y. H. Yu and J. S. Gao, *Polyhedron*, 2019, **167**, 85–92.

7 H. G. Hao, Y. C. Wang, S. X. Yuan, D. M. Chen, D. C. Li and J. M. Dou, *Inorg. Chem. Commun.*, 2018, **98**, 120–126.

8 R. Lv, J. Wang, Y. Zhang, H. Li, L. Yang, S. Liao, W. Gu and X. Liu, *J. Mater. Chem. A*, 2016, **4**, 15494–15500.

9 N. Abdollahi and A. Morsali, *Anal. Chim. Acta*, 2019, **1064**, 119–125.

10 H. Jin, J. Xu, L. Zhang, B. Ma, X. Shi, Y. Fan and L. Wang, *J. Solid State Chem.*, 2018, **268**, 168–174.

11 L. Fan, Z. Liu, Y. Zhang, D. Zhao, J. Yang and X. Zhang, *Inorg. Chem. Commun.*, 2019, **107**, 107463.

12 A. Maji, P. Majee, D. K. Singha, A. K. Ghosh, S. K. Mondal and P. Mahata, *J. Photochem. Photobiol. A Chem.*, 2018, **365**, 125–132.

13 F. H. Zhao, W. Y. Guo, S. Y. Li, Z. L. Li, X. Q. Yan, X. M. Jia, L. W. Huang and J. M. You, *J. Solid State Chem.*, 2019, **278**, 120926.

14 Y. J. Yang, D. Liu, Y. H. Li and G. H. Cui, *J. Solid State Chem.*, 2019, **278**, 120891.

15 X. Du Zhang, Y. Zhao, K. Chen, Y. F. Jiang and W. Y. Sun, *Chem. - An Asian J.*, 2019, **14**, 3620–3626.

16 X. Y. Guo, Z. P. Dong, F. Zhao, Z. L. Liu and Y. Q. Wang, *New J. Chem.*, 2019, **43**, 2353–2361.

17 J. Y. Zou, L. Li, S. Y. You, H. M. Cui, Y. W. Liu, K. H. Chen, Y. H. Chen, J. Z. Cui and S. W. Zhang, *Dye. Pigment.*, 2018, **159**, 429–438.

18 J. Zhang, L. Gong, J. Feng, J. Wu and C. Zhang, *New J. Chem.*, 2017, **41**, 8107–8117.

19 X. M. Kang, X. Y. Fan, P. Y. Hao, W. M. Wang and B. Zhao, *Inorg. Chem. Front.*, 2019, **6**, 271–277.

20 Z. Q. Yao, G. Y. Li, J. Xu, T. L. Hu and X. H. Bu, *Chem. – A Eur. J.*, 2018, **24**, 3192–3198.

21 S. Z. Wen, W. Q. Kan, L. L. Zhang and Y. C. He, *Cryst. Res. Technol.*, 2017, **52**, 1700105.

22 H. He, Q. Q. Zhu, C. P. Li and M. Du, *Cryst. Growth Des.*, 2019, **19**, 694–703.

23 T. Wiwasuku, J. Boonmak, K. Siriwong, V. Ervithayasuporn and S. Youngme, *Sensors Actuators, B Chem.*, 2019, **284**, 403–413.

24 C. S. Cao, H. C. Hu, H. Xu, W. Z. Qiao and B. Zhao, *CrystEngComm*, 2016, **18**, 4445–4451.

25 X. H. Zhou, L. Li, H. H. Li, A. Li, T. Yang and W. Huang, *Dalton Trans.*, 2013, **42**, 12403–12409.

26 W. Liu, X. Huang, C. Xu, C. Chen, L. Yang, W. Dou, W. Chen, H. Yang and W. Liu, *Chem. –*

Eur. J., 2016, **22**, 18769–18776.
27 X. Y. Dong, R. Wang, J. Z. Wang, S. Q. Zang and T. C. W. Mak, *J. Mater. Chem. A*, 2015, **3**, 641–647.
28 M. Zheng, H. Tan, Z. Xie, L. Zhang, X. Jing and Z. Sun, *ACS Appl. Mater. Interfaces*, 2013, **5**, 1078–1083.
29 R. Dalapati, Ü. Kökçam-Demir, C. Janiak and S. Biswas, *Dalton Trans.*, 2018, **47**, 1159–1170.
30 Y. Zhou, H. H. Chen and B. Yan, *J. Mater. Chem. A*, 2014, **2**, 13691–13697.
31 A. J. Weerasinghe, C. Schmiesing, S. Varaganti, G. Ramakrishna and E. Sinn, *J. Phys. Chem. B*, 2010, **114**, 9413–9419.
32 J. Wang, J. R. Wang, Y. Li, M. Jiang, L. W. Zhang and P. Y. Wu, *New J. Chem.*, 2016, **40**, 8600–8606.
33 C. Q. Zhang, Y. Yan, Q. H. Pan, L. B. Sun, H. M. He, Y. L. Liu, Z. Q. Liang and J. Y. Li, *Dalton Trans.*, 2015, **44**, 13340–13346.
34 B. Wang, Q. Yang, C. Guo, Y. X. Sun, L. H. Xie and J. R. Li, *ACS Appl. Mater. Interfaces*, 2017, **9**, 10286–10295.
35 M. Wang, J. G. Wang, W. J. Xue and A. X. Wu, *Dyes Pigm.*, 2013, **97**, 475–480.
36 S. G. Chen, Z. Z. Shi, L. Qin, H. L. Jia and H. G. Zheng, *Cryst. Growth Des.*, 2017, **17**, 67–72.
37 J. N. Hao and B. Yan, *New J. Chem.*, 2016, **40**, 4654–4661.
38 T. Q. Song, J. Dong, H. L. Gao, J. Z. Cui and B. Zhao, *Dalton Trans.*, 2017, **46**, 13862–13868.
39 H. M. He, S. H. Chen, D. Y. Zhang, R. Hao, C. Zhang, E. C. Yang and X. J. Zhao, *Dalton Trans.*, 2017, **46**, 13502–13509.
40 G. Wen, M. Han, X. Wu, Y. Wu, W. Dong, J. Zhao, D. Li and L. Ma, *Dalton Trans.*, 2016, **45**, 15492–15499.